STATUS REPORT ON RFSC ANU

N.R. Lobanov[#] and D.C. Weisser, Nuclear Physics Department, Research School of Physical Sciences and Engineering, Australian National University, ACT, Canberra 0200, AUSTRALIA

Abstract

ANU superconducting LINAC for heavy ions continues to evolve. Part of the R&D work was successfully completed and the stage one of the LINAC medium section is operating. In the second stage of the project, nine SLRs will be re-plated [1] and three more SLRs added. Further stages will involve the installation of low β, additional medium β and high β resonators. Superconducting structure development at ANU is aimed at improving the cost/performance of low/medium velocity structures for future ANU Linac upgrades. Some general features of the design of accelerator structures are outlined and designs for 150 MHz β=0.065, 0.1, 0.15 resonators are discussed. In developing the stage one of ANU Linac, a primary technical challenge was to maintain RF phase control of SLRs. This was achieved in two ways: first, the gas helium pressure was stabilized to within 25 mBar; second, the ANU ASI control units were upgraded to achieve much more stable operation.

1 INTRODUCTION

Two types of superconducting cavities have been used as a prototype for ANU LINAC upgrade. The first is the coaxial quarter-wave resonator proposed by Ben-Zvi and Brennan [2]. Due to single drift tube, the QWR has a wide transit time factor but at the price of a small voltage gain per resonator. The second is the half-wave resonator with two loading arms with straight inductors rather than curved ones of the split-ring [3]. The split-ring has loading arms of relatively small cross-section bent in circular shapes, which put limitations on the mechanical stability and on the peak surface magnetic field.

The major design criteria for our work are given by the following:

a. A structure should be simple to manufacture and balance electrically.
b. Low values of peak surface electrical and magnetic fields.
c. The frequency of lowest mechanical mode should be high.
d. Elimination of the electron-beam welds is necessary. Exclusion of brazing joint is desirable.
e. The structures should be appropriate for both niobium sputtering and lead plating.
f. The sensitivity to gas helium pressure variation should be low.
g. The temperature stabilization of the superconducting film should be efficient.

2 LOW BETA CAVITIES

Three Stub Half Wave Resonator (3SHW) and Interdigital Half Wave Resonator (IHW). Figure 1 shows 4 gap β=0.065 accelerating structure (hereafter

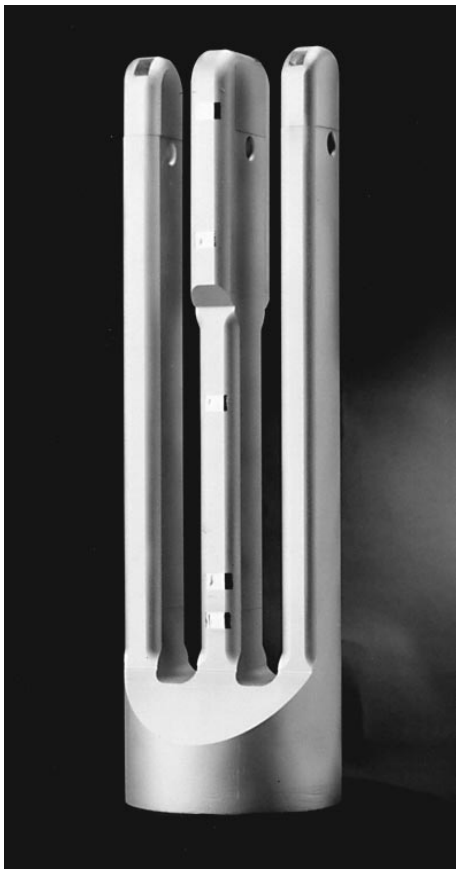

Figure 1: 4-gap β=0.065 3-stub resonator. Beam aperture is 1.8 cm and an active length is 19.4 cm

referred to as the 3-stub resonator, 3SHW). The IHW is similar to the ANL Interdigital low-beta resonator [4] (figure 2) but is based on a half wave structure rather than a quarter wave one. The half wave

[#] E-mail: Nikolai.Lobanov@anu.edu.au

resonator structure (HWR) is inspired by the Delayen design [3]. In both designs the outer cylindrical housing has an ∅=19.4 cm ID and an overall length of 59.5 cm. The center conductor has a diameter of 16.0 cm at the shorted end and splits to three stubs at the high-voltage end in 3SHW. In IHW the first inductor is terminated by forked drift tube which straddles a single drift tube sitting on the second inductor. The drift tube dimension is larger than required to shape the field on the beam axis in order to provide a large capacitive load and shorten the transmission line to increase mechanical stability.

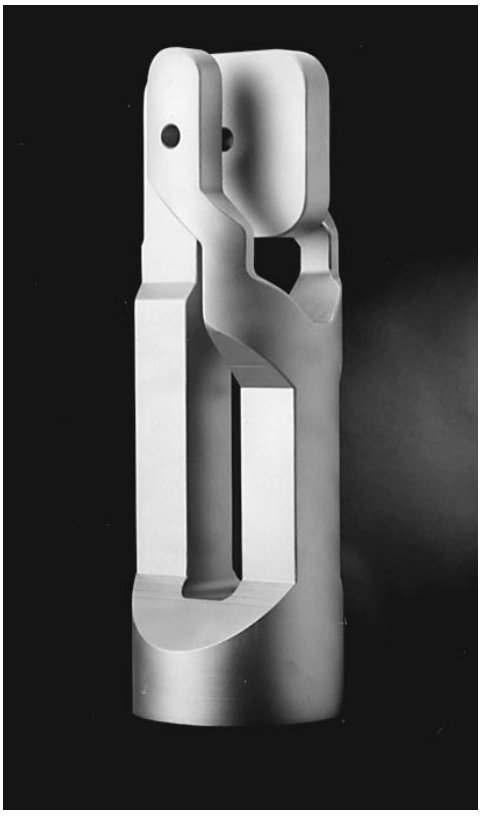

Figure 2: 4-gap β=0.065 interdigital half wave resonator

The 3-stub resonator has three principal RF low frequency eigen-modes: two accelerating modes in which charge oscillates between the beam drift tubes and a quarter wave mode in which charge oscillates between the drift tubes and the outer wall. Similarly the IHW has two oscillating modes. In the ideal HWR running in acceleration mode, no net RF current passes between the stubs and the outer wall which minimizes joint losses. The efficiency of the accelerating mode becomes maximum for a spacing at which the central gap between drift tubes is approximately twice the end gap [5]. At maximum efficiency, effects of vibration induced motion of the structure is minimized due to cancellation of coupling between mechanical vibration mode of the stubs and the electric field [5]. Imbalance in the stub configuration can produce coupling between the accelerating and quarter wave modes. This causes net RF current through the RF joint at the base of the outer wall increasing joint losses. The design shown in figures 1 and 2 minimizes this problem by splitting the non-accelerating or quarter wave mode to lower frequency by ~15 MHz.

Table 1 compares the electromagnetic properties of the low beta 3SHW and IHW with the QWRs and half wave resonator. The peak surface fields are acceptably low, and the performance should be limited by field emission.

3 MEDIUM AND HIGH BETA CAVITIES

3.1 Quarter Wave Resonators

A design is similar to concept reported in [6]. The main feature is the absence of the donut-shaped drift tube, replaced by a hole through the inner conductor. The beam ports are located outside the outer wall and joined by indium gaskets minimising the number of brazed joints. A taper could reduce the maximum magnetic field just by 25%. A straight shape of inner electrode is less affected by multipacktoring but has a lower value of shunt impedance. The resonator has a curved shorting plate which, together with the straight stub, enables better results both for coating and surface preparation.

A medium beta QWR was built in aluminium for experimental modelling, which is shown in figure 3. The electromagnetic QWRs characteristics for both medium and high beta QWRs based on Superfish calculations are presented in Table 1.

Table 1: Parameters of ANU 150 MHz resonators.

Parameter	3 Stub	Inter-digital	QWR β_{10}	Half Wave	QWR β_{15}
β_{opt}	0.065	0.065	0.11	0.1	0.15
Γ, Ω	16 [e]	33 [e]	21 [f]	17 [e]	27 [f]
R'_{sh}, MΩ/m [a,b]	15 [d]	13 [d]	25 [f]	15 [d]	40 [f]
U/E_a^2,mJ/MV/m^2	32 [d]	42 [d]	13 [f]	37 [d]	24 [f]
E_p/E_a [b]	3.8 [f]	3.8 [f]	3.1 [f]	3.3 [f]	4.0 [f]
H_p/E_a, G/MV/m [b]	59 [d]	61 [d]	53 [f]	57[d]	61 [f]
f_{mech}, Hz	88	120	140	120	140
Q_0 [a)]	4,075 [a,e]	10,539 [a,e]	6,277 [f]	4,174 [a,e]	8,565 [f]

[a)] For aluminium at 300K (R_s=4 mΩ); [b)] Neglecting transit time effect; [d)] Calculated from Ref.[2];
[e)] Experimental; [f)] Calculated with Superfish

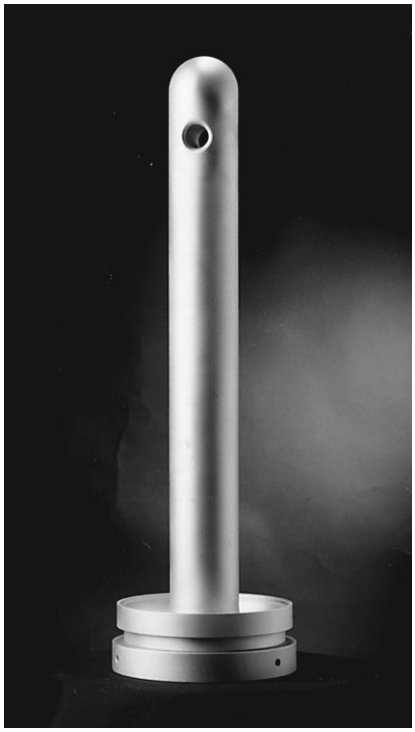

Figure 3: 150 MHz QWR for the booster LINAC at ANU

Figure 4: Half Wave Resonator for β_{opt} =0.1

3.2 Half Wave Resonator

The resonator grows from the design reported previously [3], figure 4. The displacement current needed to establish the 150 MHz voltage on the drift tubes is carried between them by a balanced inductive loop. The HWR has two principal low frequency eigen-modes similar to those described in section "3SHW and IHW". The oscillating loop is mounted within a cylindrical outer wall with ∅=19.4 cm I.D. and an overall length of 60.0 cm closed with tuner plate.

The mechanical and electromagnetic properties of HWR are shown in Table 1. The balanced field profile is achieved by selective machining of the inductors. A straight shape of inductors is expected to minimize multipacktoring and, together with curved shorting plate, provide better conditions for coating and surface preparation.

3.3 Accelerating field profile. Peak Surface Electric Field.

The drift tube geometry was derived with a help of Superfish/Poisson solving electrostatic problem with cylindrical symmetry. Electrostatic geometry for a one, two and three-stub structures was generated as recommended in [7]. The quantities obtained are surface fields on the conductors, peak surface electric field (see table 1), and field distribution on the beam line.

3.4 Shunt Impedance. Energy Content. Peak Surface Magnetic Field

Q_0 value can be used to infer the geometry factor through the general resonator relationship $\Gamma=Q_0R_s$, where $R_s\approx4$ mΩ is the surface resistance of aluminium at 150 MHz and 300K. A set of expressions for the electromagnetic properties of low velocity accelerating structures based on quarter-wavelength resonant lines [2,7] was used to derive the values of R'_{sh}, U/E_a^2 and H_p/E_a given in table 1. The radius of outer wall *b* used in all equations from [2,7] is chosen to get a good fit for the geometry factor $\Gamma_{(b,a)}$ since b is not well defined in non-symmetric devices.

3.5 Mechanical Stability

Response of the mechanical structure to environmental noise determines the frequency stability, which can be characterized by the eigenfrequency of mechanical vibration f_m [9]. The eigen-frequency of OHFC copper beam of uniform section and uniformly distributed load anchored at one

end is given by $f_{mech}[Hz]=2.036x10^{5}I^{0.5}A^{-0.5}L^{-2}$, where $I_{[cm^4]}$ is the area moment of inertia of beam cross section A, cm^2 and L is the length, cm [10]. For a solid stub of length of about 45-48 cm, all modes are above 88 Hz so there is no necessity of using fast tuners [11] or in lowering of the mechanical quality factor [12].

3.6 RF Joints

Proposed accelerating structures have one joint for the outer wall to the shorting plate and one joint for the tuner plate to the outer wall. In both cases, the current density is not high. All cavities have the central "T" piece made of OHFC. In QWRs, the "T" shaped central conductor is UHV brazed to the external cylinder. UHV brazing has been shown to be equivalent to EBW [13]. An alternative technique consists of excavating the full resonator by machining an OHFC billet and by backward extrusion of a short billet [14]. In our case, it is essential to eliminate the EBW of copper because convenient EBW facility is not available in Australia and EBW often results in unavoidable micro-cracks, craters and material projections in the joint.

Low loss disassemble joints for Nb resonators have been developed at ANL and JAERI. If a low loss disassemble joints can be developed for these resonators, the fabrication would be greatly simplified especially in the half wave group (3SHW, IHW and HW) where charge oscillates between drift tubes. Lead wire and indium-tin both gave good results in SLRs [5,17]. In [18] thermometry measurements demonstrated that, in the absence of field emission, only about 5% of the total 4.2K losses occur on the resonator outer housing. The estimated values of RF losses in the gasket for half wave-type resonators described above are less than in SLRs.

4 NIOBIUM ON COPPER

The research program of sputtered Nb/Cu QWRs continues to be pursued employing magnetron sputtering. Two QWRs were sputtered and achieved moderate Q. These are used as a superbuncher in 1992 and Time Energy Lens in 1997. The progress in R & D up to 1997 was reported in [19]. Due to many other activities, there was no Nb sputtering on QWRs since the last RFSC workshop. Currently one QWR is being prepared by tumbling, polishing and brazing of the ‘doughnuts”. The magnetron cathode (figure 5) has been modified for Nb sputtering.

Modification involved improvements of the structural stability of the cathode by introduction of spring-loaded support legs. The skeleton of the device was

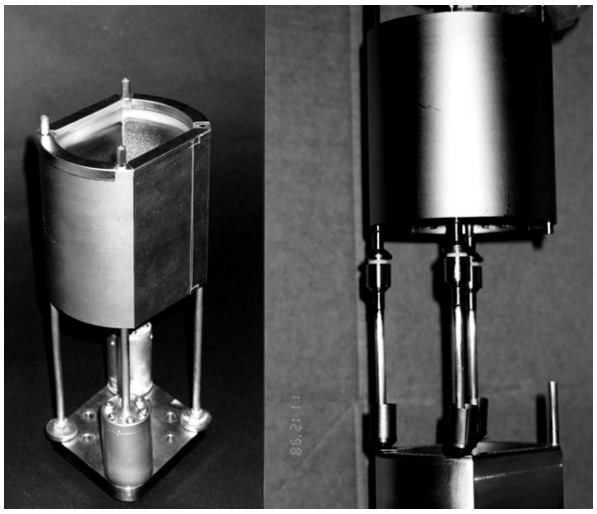

Figure 5: Magnetron sputtering cathode after modification.

subject to slight misalignment caused by thermal gradients.

5 GAS HELIUM PRESSURE STABILIZATION

The slow variation of the pressure in the return helium gas space has been identified as dominant source of mechanical noise affecting the frequency stability of SLRs. Liquid helium produced by the Sulzer TCF50 liquifier is delivered into the 450 l dewar at the pressure 1.26-1.30 bar absolute. To deliver liquid helium into the cryostats, the pressure in the dewar has to be increased to produce a 0.25 bar pressure difference between the delivery and the return manifolds of the distribution system. This is achieved by restricting the return flow valve from the dewar controlled by the pressure difference. The pressure variation has been maintained within 25 mBar by stabilizing the absolute pressure in the return path of the distribution system. This reduced the frequency shift to less than 40 Hz and just overcoupling was sufficient to keep the resonators locked.

A new computer controlled function has been defined which operates a proportional valve on the distribution return path where it joins gas from the dewar entering the liquefier. The core part of the LINAC cryogenic process control is a SattCon 31-10 PLC, which reached its limitations. A more modern and larger capacity system is being installed to cater for future expansion.

6 LINAC RF CONTROL SYSTEM UPGRADE

The interaction of SLRs reported in [9] was caused by crosstalk via the RF switch box use for monitoring field in resonators. The problem was solved by replacing the RF box with individual RF channels.

During operation a 1% field amplitude drift of SLRs was noticed. The time period of the drift was approximately 6.5 minutes. Upon further investigation the period was shown to be the ambient air temperature cycle of LINAC hall T_{amb}=20.4±0.8 °C. ASI RF control boxes are now being upgraded with the electronic thermostat with the idea of having a highly stable temperature inside the box at T_{ASI}=36.0±0.05 °C. This should reduce temperature associated amplitude drift to less than 0.1%.

7 LINAC SLRs REPLATING

A detailed account for the lead plating can be found elsewhere in these proceedings [1].

8 CONCLUSION

Several 150 MHz resonators were designed and built from aluminium using wire cutting equipment. An experimental and theoretical procedure to optimize the design of these structures was also presented. The fabrication of resonators was greatly simplified by using spark-erosion process and disassemble RF joint between "T"-shaped central electrode and external wall. Fabrication of the OHFC resonators is expected after completion of re-plating ANU LINAC SLRs in late 2000.

9 ACKNOWLEGEMENT

The competence and the skill of the staff of ANU have been a key issue for the advancement of the project. The authors would like to thank mechanical workshop ANU for their cooperation, skill and enthusiasm during this work and for operation of spark-erosion machine to build full-scale aluminium resonators.

10 REFERENCES

[1] N. Lobanov and D.Weisser, "Lead Plating:ANU SLRs Upgrade" to be published in in Proceedings of the 9th Workshop on RF Superconductivity, Santa Fe, November 1999.
[2] I.Ben-Zvi and J.Brennan, Nuclear Instruments and Methods, 212, 73-79 (1983).
[3] J.Delayen and J.Mercereau, Nuclear Instruments and Methods in Physics Research, A 257, 71-76 (1987).
[4] K.W.Shepard, IEEE Transactions on Nuclear Science, Vol.NS-32, N5 (1985) 3574-3577.
[5] J.Delayen, G.Dick and J.Mercereau, IEEE Transactions on Magnetics, vol. MAG-17, N1 (1981), 939 942.
[6] V.Palmieri et.al, Nuclear Instruments and Methods in Physics Research, A 382, 112-117 (1996).
[7] J.R.Delayen, Nuclear Instruments and Methods in Physics Research, A 259, 341-357 (1987).
[8] E.L.Ginzton, Microwave Measurements, NY, 1957, pp.435-445.
[9] N.Lobanov and D.Weisser, "Linac Boosters- An Overview", *in Proceedings of HIAT98,* (K.Shepard, ANL), AIP, 1999, pp.117-137.
[10] C.Harris and C.Crade. Shock and Vibration Handbook, vol.1, NY, 1976.
[11] V.Zviagintsev, V.Andreev, A.Facco, in *Proceedings of the 8th Workshop on RF Superconductivity,* (V.Palmieri ed., Abano Terme 1997), 1999, vol.3, pp. 695-700.
[12] A.Facco, in 8th RFSC, V.Zviagintsev, V.Andreev, A.Facco, in *Proceedings of the 8th Workshop on RF Superconductivity,* (V.Palmieri ed., Abano Terme 1997), 1999, vol.3, pp. 685-693.
[13] R.Pengo et.al., Cryogenics, vol.30, 1990, pp.74-76
[14] V.Palmiery, in *Proceedings of the 8th Workshop on RF Superconductivity,* (V.Palmieri ed., Abano Terme 1997), 1999, vol.3, pp. 553-589.
[15] T.Yogi, Cryogenics (1973), p.369.
[16] D.W.Storm, J.M.Brennan, I.Ben-Zvi, IEEE Trans. on Nucl.Sci., NS-32 (1985), p.3607.
[17] J.Noe, in *Proceedings of the HIAT98,* (K.Shepard, ANL), AIP, 1999, pp.192-213.
[18] J.W.Noe et. al., *in Proceedings of the 6th Workshop on RF Superconductivity,* (ed., R.Sundelin), 1993, pp.1052-1064.